Princeton Plasma Physics Laboratory

NSTX Experimental Proposal

Title: HHFW Current Drive Experiment

OP-XP-403	**Revision:**	Effective Date: *(Ref. OP-AD-97)* Expiration Date: *(2 yrs. unless otherwise stipulated)*

PROPOSAL APPROVALS

Author: P. M. Ryan, D. W. Swain, J. R. Wilson	Date
ATI – ET Group Leader: G. Taylor	Date
RLM - Run Coordinator: S. M. Kaye	Date

Responsible Division: Experimental Research Operations

Chit Review Board (designated by Run Coordinator)

MINOR MODIFICATIONS (Approved by Experimental Research Operations)

NSTX EXPERIMENTAL PROPOSAL

HHFW Current Drive Experiment OP-XP-403

1. Overview of planned experiment

Maintenance of plasma current by non-inductive means represents one of the most important mission elements of the NSTX Program and is of common interest to magnetic fusion energy sciences research. High power HHFW with an increased wavelength in the direction of the magnetic field via flexible control will be launched with a fast propagation velocity along the magnetic field line. This wave is expected to maximize momentum transfer to the electrons and drive plasma current non-inductively, while applying strong heating to increase plasma pressure and self-driven (bootstrap) current. The efficiency of combined HHFW-driven and self-driven current will be estimated by comparing global measurements in modest current plasmas with theory. An understanding of the underpinning physics of HHFW and self current drive and the techniques to ensure reliable operation at high power levels will contribute to future investigation of spherical torus plasmas sustained for longer durations in NSTX.

We propose to build upon the current drive results obtained in 2002 and 2003 by operating the HHFW CD array at higher rf powers, higher electron temperatures, and higher wave phase velocity (lower $k_{||}$). We intend to operate at time-invariant plasma conditions sufficiently long to unambiguously measure the effects of driven current by the external magnetics (reduced loop voltage). The time constant is expected to be on the order of 100 ms. The experiment aims to establish the current drive efficiency scaling with respect to density, electron temperature, and $k_{||}$. This information is needed for extrapolation to advanced integrated scenarios.

2. Theoretical/ empirical justification

Figure 1 shows the CD efficiency obtained on NSTX at $k_{||} = 7.6\ \mathrm{m}^{-1}$ in comparison with the fast wave current drive results from DIII-D (C. Petty) and TFTR. The DIII-D antenna array has fixed relative phasing (fixed $k_{||}$) but variable frequency; hence the wave velocity can be increased by increasing the frequency. On DIII-D the normalized current drive efficiency was higher for 117 MHz operation than for 60 MHz. On NSTX the frequency is fixed for the HHFW array, but the relative phasing can be varied; the wave phase velocity can be increased by decreasing $k_{||}$. The goals of this XP are to obtain CD data at higher electron temperatures and higher wave velocity, and to verify the density scaling.

Figures 2 and 3 show calculated current drive efficiencies for two different toroidal wave numbers, 7.6 and 3 m^{-1}, as the electron density and temperature are changed; the calculations were made with the ray-tracing code CURRAY (T. K. Mau) and the full-wave code AORSA (E. F. Jaeger). The base shot for the scaled density and temperature profiles is 110145; the parameters used are $B_0 = 0.45$ T, $I_p = 0.5$ MA, $T_i/T_e = 0.7$, and a deuterium plasma with a 4% hydrogen minority fraction. Experimental points for 7.6 m^{-1} operation are included for comparison. The wave velocity for $k_{||} = 8\ \mathrm{m}^{-1}$ corresponds to an 800 eV electron thermal velocity, while $k_{||} = 3\ \mathrm{m}^{-1}$ corresponds to $T_e = 4$ keV. Simple theory predicts wave interactions with the electrons when the wave velocity is 0.5 to 2.0 times the thermal velocity, with higher efficiency corresponding to the higher velocity ratio. However, the calculations also show more off-axis power deposition for the higher wave velocity, which cannot be explained by wave-particle velocity matching and depends on the ray trajectories for power propagation. Little power (< 6%) is absorbed by minority ions at 7.6 m^{-1} even at the highest temperatures, while 3 m^{-1} operation is predicted to deposit up to a third of the power on minority ions at high ion beta. Still, the current drive efficiency at 3 m^{-1} is calculated to exceed that at 7.6 m^{-1} in every case considered.

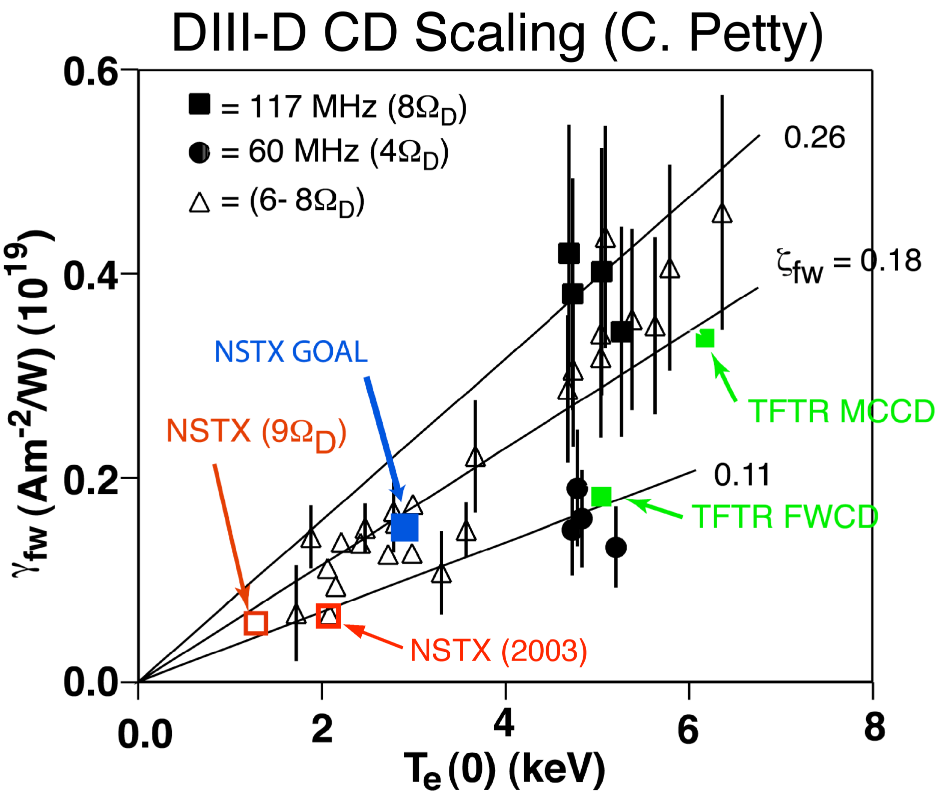

Fig. 1 Normalized CD efficiency vs Te for DIII-D, TFTR, and NSTX.

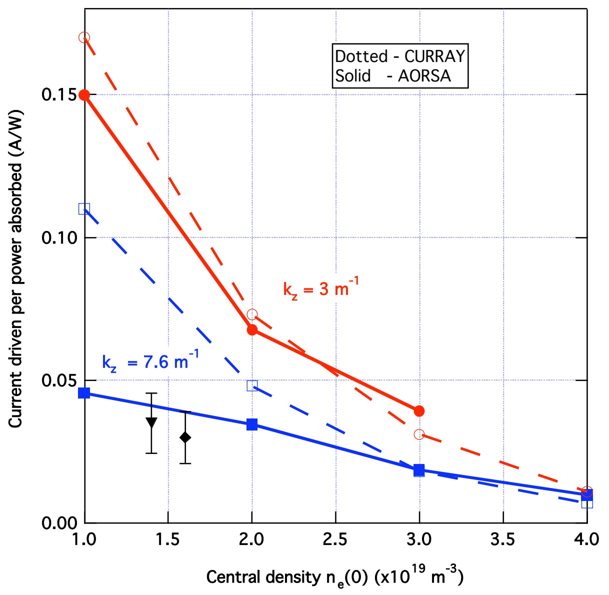

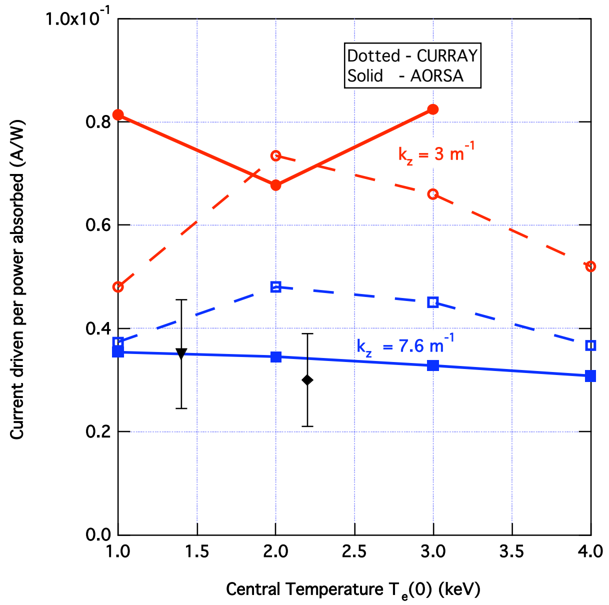

Fig. 2 Density scan at constant temperature ($T_e(0)$ = 2 keV)

Fig. 3 Temperature scan at constant density ($n_e(0)$ = $2x10^{19}$ m^{-3})

Some of the operational problems encountered in 2002 were improved during 2003 operation; these still will need to be checked early in the 2004 campaign.

1. HHFW Power limitations
A voltage limit of ~13 kV (as measured at the feedpoint of the resonant loops) restricted operation to less than 3 MW for co-CD phasing and 1.5 MW for counter-CD phasing in 2002. It is believed that this was primarily due to arcing in the vacuum feedthroughs of the antenna straps. Subsequent modification of the feedthroughs permitted routine, reliable operation in 2003 above 4 MW for co-CD and 2 MW in counter-CD. RANT3D calculations indicate that the antenna loading for –30° relative phasing (k_z = -3 m^{-1} for co-CD) will be similar to the loading for –90° phasing (k_z = -7.6 m^{-1} for co-CD): 11 Ω and 10 Ω, respectively. The same analysis gives loading of 7 Ω for +30° vs 4 Ω for +90°. This suggests that reliable power levels of 4-5 MW for –30° phasing and 3 MW for +30° phasing may be achievable. These loading predictions will need to be checked during HHFW conditioning operations.

2. RF Noise pickup in the plasma control positioning coils.
In 2002 rf noise pickup in the plasma position coils increased as the rf power increased and as the array phase angle decreased, to the point that plasma position control became difficult above about 2 MW. Increased shielding and filtering of the signal integrators are expected to alleviate this problem. This also needs to be checked during HHFW conditioning operations.

3. MHD activity during the rf application
MHD instabilities encountered when q(0) approached unity (and the concomitant central temperature collapses) were observed to reduce the non-inductive driven current. A low l_i, high q(0) discharge with good MHD stability during the current flat-top is needed to measure the effects of HHFW CD on the loop voltage. Early application of the rf pulse (t = 0.075 s) at somewhat reduced power (~ 1.5 MW) was found to keep q(0) above unity for 500-600 msec in 2003 operation.

4. No measurement of current drive profiles

The absence of the Motional Stark Effect diagnostic has prevented current density profiles from being measured during our CD experiments. The HHFW driven current can be estimated by establishing identical plasma conditions for co-CD and counter-CD phasing and assuming:

1. Steady-state (t > L/R) conditions have been achieved.
2. The plasma ohmic resistance is the same for both co- and counter-CD phasings.
3. The HHFW driven current is proportional to the rf power.

Under these assumptions a 0D calculation of the driven current can be made from the measured loop voltage, after subtracting the calculated bootstrap current and compensating for the portion of the loop voltage that drives the changing magnetic stored energy. This analysis will continue to be used. If the MSE diagnostic becomes operation during the latter stages of the 2004, this experiment may be repeated. Moreover, improvements in EFIT analysis may yield current profiles that are sufficiently accurate to detect the rf-driven current.

3. Experimental run plan

This XP is a continuation and completion of XP-312; only the first day of XP-312 was carried out in 2003. We scanned the power from 2-4.5 MW in the co-CD direction (-90° phasing) and from 1-2.3 MW in the counter-CD direction (+90° phasing). The central electron temperature reached as high as

2.3 keV. The current drive efficiency was essentially the same as that achieved in 2002 at lower temperature ($T_e(0) \sim 1.5 – 1.7$ keV). This temperature scaling agrees with the 7.6 m^{-1} prediction in Fig. 3.

We also operated at 60° relative phasing, where the power is equally divided between peaks at 7.6 and 3 m^{-1} (see Fig. 4). The motivation was to heat the electrons with the slower waves until they were hot enough to interact efficiently with the faster waves. Operation at –60° was indistinguishable from –90° as far as electron temperature and loop voltage were concerned.

XP-403 will address the second part of the original XP-312: current drive operation at $k_{||} = \pm 3\ m^{-1}$.

Operation will be in He for better density control and to avoid H-mode. We will use lower single null plasmas unless double null plasmas have already demonstrated superior HHFW results (update: shot 111394 has been established as good target shot). Most operation will be at low density to maximize the driven current; some operation at higher density to establish scaling. We will start with ±30° phasing so as to ensure that 3 m^{-1} operation is attempted during the run day. We will finish with ±90° phasing for comparison with both ±30° and previous ±90° experiments.

Shot list (**34 GOOD shots**):

1. Power scan at –30° phasing (2, 3, 4, 5 MW), low density ($n_{e0} \sim 1\text{-}1.5\times10^{19}\ m^{-3}$). Repeat one shot with CHERS NBI blip. (**5 shots**)
2. Ohmic only shot. (**1 shot**)
3. Power scan at +30° phasing; adjust gas feed to match step 1 density if needed. Repeat one shot with CHERS NBI blip. (**5 shots**)
4. Ohmic only shot. (**1 shot**)
5. Power scan at –90° phasing (2, 3, 4, 5 MW), low density ($n_{e0} \sim 1\text{-}1.5\times10^{19}\ m^{-3}$). Repeat one shot with CHERS NBI blip. (**5 shots**)
6. Ohmic only shot. (**1 shot**)
7. Power scan at +90° phasing; adjust gas feed to match step 3 density if needed. Repeat one shot with CHERS NBI blip. (**5 shots**)
8. Ohmic only shot. (**1 shot**)
9. Power scan (2, 3, 4, 5 MW) at symmetric phasing (00ππ00, ±7.6 m^{-1}) Repeat one shot with CHERS NBI blip. (**5 shots**)
10. Increase density ($n_{e0} \sim 2\text{-}2.5\ \times10^{19}\ m^{-3}$) and take –30° shot at the highest power achieved in Step 1. Repeat for +30°. (**2 shots**)
11. Repeat step 10 for ±90°. (**2 shots**)
12. Ohmic only shot (**1 shot**)

Contingency if Step 1 fails to heat electrons:

1-alt. Initial heating at –90°, then switch to –30° after $T_{e0} > 1$ keV.

a) Check matching for these two phasings during array conditioning XMP, to determine if step b is feasible.

b) Match for –30° and initially heat at –90° at reduced power (< 2MW), accepting large reflected power during the mismatch. Switch to –30°, matched operation when $T_{e0} > 1$ keV.

2-alt. If step 1-alt doesn't work, apply NBI early in the pulse to heat electrons. Overlap NBI and RF by ~20 ms.

3-alt. Repeat step 1-alt or step 2-alt for +30° phasing. If neither has worked, go to step 3 above (±90° operation).

4. Required machine, NBI, RF, CHI and diagnostic capabilities

Prior to experiment:

Check the noise immunity of plasma positioning and control system (and diagnostics) for low array phase shift operation.

Check the loading and the matching requirements for ±30° and ±90° operation.

Ascertain the voltage/power limits of the HHFW system.

Establish an MHD-stable, low-density LSN plasma shot for reference target.

Machine will be operating at $I_p \sim 500$ kA, $B_T \sim 0.45$ T, He, for long (~ 1 s) pulses.

The RF system needs all six transmitters operating for long pulses at 600-750 kW each, phase control feedback, and I-V cube signals (phase and magnitude).

NBI (source A) should be prepared to operate if needed (80 kV, D, ~ 100 ms)

Need Thompson scattering system for T_e, n_e profiles, microwave reflectometer for edge density profiles, magnetics for EFIT equilibrium calculations, edge rotation diagnostic for ion interaction, and Plasma TV for antenna hot spot surveillance. CHERS (for 1-2 shots), X-ray crystal desirable for T_i measurements, soft X-ray array and GEMS for temperature/power deposition information, and spectroscopy for Z_{eff} measurements (Z_{eff} profile would be desirable).

5. Planned analysis

EFIT analysis for internal inductance, surface voltage, and q-profile; TRANSP analysis for bootstrap current, parallel electric fields and driven current. Experimental measurements will be used to benchmark predictions of ray-tracing codes (CURRAY, HPRT, CQL3D) and full-wave codes (TORIC, AORSA).

6. Planned publication of results

Preliminary results will be presented at the EPS and/or APS meetings. Eventual publication in peer reviewed journal will follow MSE measurements of current profiles.

PHYSICS OPERATIONS REQUEST

HHFW Current Drive Experiment **OP-XP-403**

Machine conditions (specify ranges as appropriate)

I_{TF} (kA): **52 kA (4.5 kG)** Flattop start/stop (s): _____/_____

I_P (MA): **500 kA** Flattop start/stop (s): **.150 / .900**

Configuration: **Lower Single Null**

Outer gap (m): **0.05**, Inner gap (m): **0.05**

Elongation κ: _____, Triangularity δ: _____

Z position (m): **0.00**

Gas Species: **He**, Injector: **Midplane**

NBI - Species: **D**, Sources: **A/B/C**, Voltage (kV): _____, Duration (s): **0.1**

ICRF – Power (MW): **2-5** , Phasing: **CD**, Duration (s): **0.7**

CHI: **Off**

Either: List previous shot numbers for setup: **111394**

Or: Sketch the desired time profiles, including inner and outer gaps, κ, δ, heating, fuelling, etc. as appropriate. Accurately label the sketch with times and values.

DIAGNOSTIC CHECKLIST

HHFW Current Drive Experiment **OP-XP-403**

Diagnostic	Need	Desire	Instructions
Bolometer – tangential array			
Bolometer array - divertor			
CHERS	✓		
Divertor fast camera			
Dust detector			
EBW radiometers			
Edge deposition monitor			
Edge pressure gauges		✓	
Edge rotation spectroscopy	✓		
Fast lost ion probes - IFLIP			
Fast lost ion probes - SFLIP			
Filtered 1D cameras			
Filterscopes			
FIReTIP	✓		
Gas puff imaging			
Infrared cameras			
Interferometer - 1 mm		✓	
Langmuir probe array		✓	
Magnetics - Diamagnetism	✓		
Magnetics - Flux loops	✓		
Magnetics - Locked modes			
Magnetics - Pickup coils	✓		
Magnetics - Rogowski coils	✓		
Magnetics - RWM sensors			
Mirnov coils – high frequency		✓	
Mirnov coils – poloidal array			
Mirnov coils – toroidal array			
MSE		✓	
Neutral particle analyzer			
Neutron measurements			
Plasma TV	✓		
Reciprocating probe			
Reflectometer – core		✓	
Reflectometer - SOL		✓	
RF antenna camera	✓		
RF antenna probe		✓	
SPRED			
Thomson scattering	✓		
Ultrasoft X-ray arrays	✓		
Visible bremsstrahlung det.		✓	
Visible spectrometers (VIPS)	✓		
X-ray crystal spectrometer - H		✓	
X-ray crystal spectrometer - V		✓	
X-ray PIXCS (GEM) camera			
X-ray pinhole camera			
X-ray TG spectrometer			